Title
Mapping of EEG to Brain MRI for Epilepsy Localization

Author
Speidel, Benjamin

Publication Date
2017

Peer reviewed|Thesis/dissertation

Mapping EEG to Brain MRI for Epilepsy Localization

by

Benjamin Speidel

THESIS

Submitted in partial satisfaction of the requirements for the degree of

MASTER OF SCIENCE

in

Biomedical Imaging

in the

[redacted]

Acknowledgments

I would like to give special thanks to Dr. Robert Knowlton for his support and guidance throughout this project. His wealth of knowledge and experience has been invaluable. I would also like to acknowledge Dr. Alastair Martin for helping navigate the road from student to scholar. Being available for advice over the course of this program has been an incredible resource. He and program director Dr. David Saloner have done an excellent job of setting up this program and providing a network of support.

I would also like to thank Dr. Edward Chang and the entire Chang lab at UCSF for providing a welcoming environment and helping me learn how this field functions on a practical level. The work they do is impressive and innovative and they took time out of their full schedule to help me learn and become adjusted to the way this great lab functions.

Finally, the entire MSBI student and faculty community deserves recognition for creating an atmosphere of collaboration and learning. We have been able to create a network of successful students because of the great instructors and the team of students willing to collaborate in order to all succeed together.

Mapping of EEG to Brain MRI for Epilepsy Localization

Ben Speidel

Accurate localization of epilepsy foci is essential prior to resection of epileptogenic zones of the brain. EEG signatures indicative of epileptic seizures can be mapped to their location on a brain MRI by acquiring the MRI before implanting the electrodes in the brain, and localizing the electrodes within the head with a CT after implantation. However, distortion resulting from the craniotomy and the implantation procedure change the brain geometry causing the frame of reference to shift and this model to be inaccurate. Using B-Spline transformations and an Advanced Mattes Mutual Information metric, a nonrigid registration was performed between CT scans before and after the implantation procedure. This transformation was subsequently applied to the MRI in order to correct for the mismatch in registration in 5 subjects. After the application of this nonrigid transformation there was an average increase in accuracy of 12.5% ± 2.3% ($p<0.001$) in the ability of depth electrodes to localize gray matter. On average, the grid electrodes were 3mm ± 3mm ($p= 0.06$) closer to their locations given by an intraoperative photograph in one patient when the transformation was applied as well. This has been incorporated into a completely automated tool that can be easily implemented into a lab or clinical environment.

Contents

List of Tables

List of Figures

1 Introduction

1.1 Background

Epilepsy is a disorder of the brain characterized by an enduring predisposition to generate epileptic seizures and by the neurobiologic, cognitive, psychological, and social consequences of this condition which afflicts 3.4 million people in the United States.[1,2] In practice, a patient must have two unprovoked epileptic seizures more than 24 hours apart from each other in order to be diagnosed with epilepsy.[3] An epileptic seizure is defined as a transient occurrence of signs and/or symptoms due to abnormal excessive or synchronous neuronal activity in the brain.[1] Many antiepileptic drugs exist to prevent these seizures. However, it is estimated that between 20 and 40 percent of patients with epilepsy will not be able to control their seizures with medication alone.[4] For these patients (approximately 1.1 million in the US) continued seizures are disabling and carry a significant cumulative risk for associated mood disorders, cognitive decline, injury and death, and other interventions need to be considered. One such consideration is the surgical resection of the epileptogenic zone of the brain for epilepsies that are focal in nature. Essential to the successful outcome of the surgery is the accurate localization of the epileptogenic focus.[5]

Abnormal electrical signals from neuronal and synaptic activity can be electrically detected at the scalp using electroencephalography (EEG). EEG is used to examine and identify epileptic patterns and localize seizures. Often, however, it is not possible to sufficiently localize seizures for surgical decision-making with scalp EEG, and more invasive procedures must be used. Electrocorticography (ECoG), a medically invasive procedure that intracranially records electric signals from the brain, does not require the signal to pass through the skull and provides

improved spatial resolution and source localization over EEG.[6] The method requires a craniotomy and direct implantation of the electrodes.

In preparation for surgery, a preoperative MRI is acquired in order to capture the high-resolution data corresponding to the patient's anatomy with detailed information on the cortical structure of the brain. For structural analysis, an inversion recovery prepared fast spoiled gradient echo sequence such as MPRAGE or BRAVO is typically used in order to obtain 3D T1 weighted images with good gray/white matter contrast. This MRI is acquired before the implantation in order to visualize the anatomy without any susceptibility artifacts that would be created by the electrodes. After the implantation procedure, a high resolution CT is obtained. This is to make sure that there are no postsurgical complications, and to visualize the location of the electrodes. The cranial anatomy given by the MRI and the sensor positions given by the CT can then form a model by which a signal can be localized. Physicians then observe these signals using clinical software that combines the anatomy given by the MRI, the sensor locations given by the CT and electrical activity recorded by the electrodes to create a model capable of determining the spatial location of the epileptic focus.

1.2 Project goals

Surgical manipulations such as tissue removal during surgery, swelling, loss of cerebrospinal fluid and other factors cause brain deformation or brain shift after neurosurgery.[7] Due to this distortion, the resulting postoperative CT images do not directly correspond to the anatomy in the preoperative MRI. This causes problems with source localization software, as localization errors tend to be higher in brain regions that deviate from the actual cranial geometry of the

patient.[8] This also renders the coordinates of the coregistered electrodes on the CT inaccurate in the anatomical space referenced in the MRI providing an invalid frame of reference. An example of this brain shift is shown in figure 1.

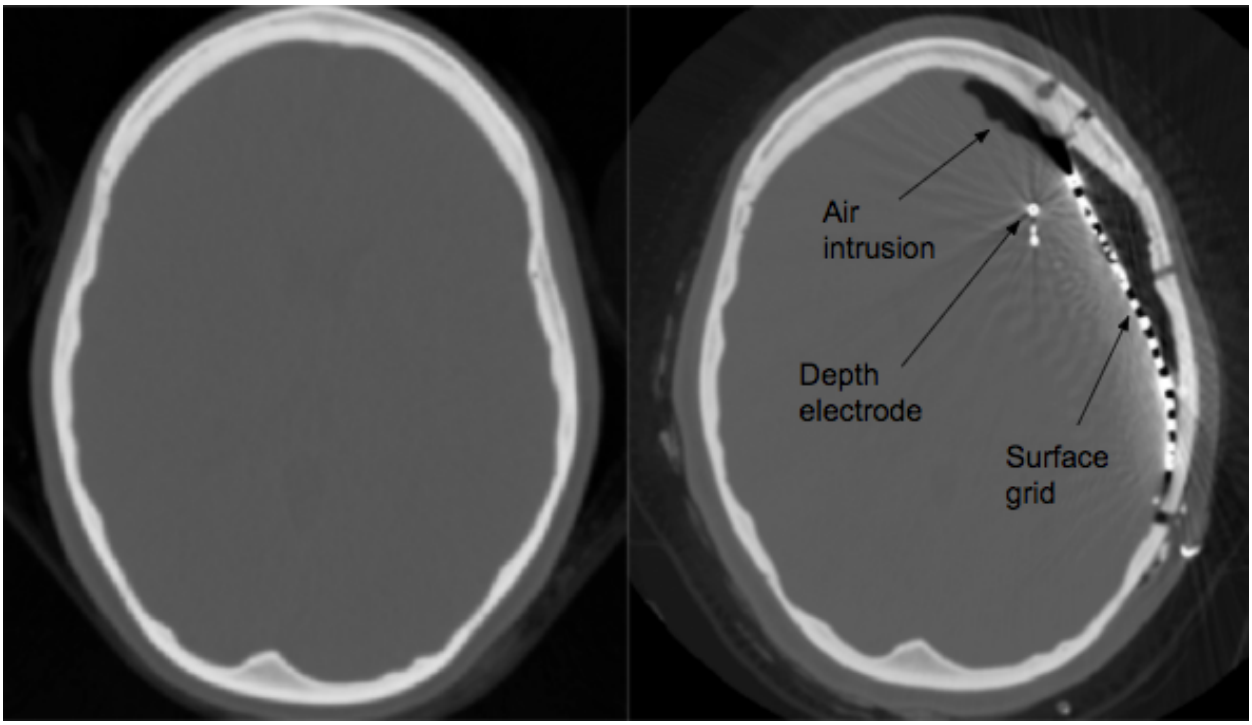

Figure 1: Shift due to electrode implantation and air in the cranial cavity. CT on the left is subject before surgery. CT on the right is the same subject after electrode implantation.

Methods have been proposed to correct for this in which the electrodes in the surface grids are manually selected on the CT, and those coordinate estimates are pulled to the dural surface of the MRI using an energy minimization algorithm. These coordinates on the dural surface are then projected to the closest vertex on the pial surface.[9] However, this method only corrects for the radial displacement of the electrodes in reference to the MRI, assuming that the correct location for each electrode is actually the nearest cortical surface without taking into account the structural information given in the two images. The energy minimization algorithm also cannot be applied to the depth electrodes, electrodes placed to sample cortex below the pial surface. As an alternative or supplement to these methods, nonrigid registration can be used to correct for

this distortion and provide more accurate localization of all intracranial electrodes. By nonrigidly registering the MRI to the CT prior to any modeling or source localization, the accuracy of the sensor locations and the model will be improved. This should prove beneficial in improving the accuracy of the epileptogenic focus localization and patient outcomes. The automated pipeline here will use B-spline transformations, take in a CT from before the implantation register it to the CT after the operation, and apply the resulting transformation to the MRI in order achieve this more accurate model.

2 Methods

2.1 Registration overview

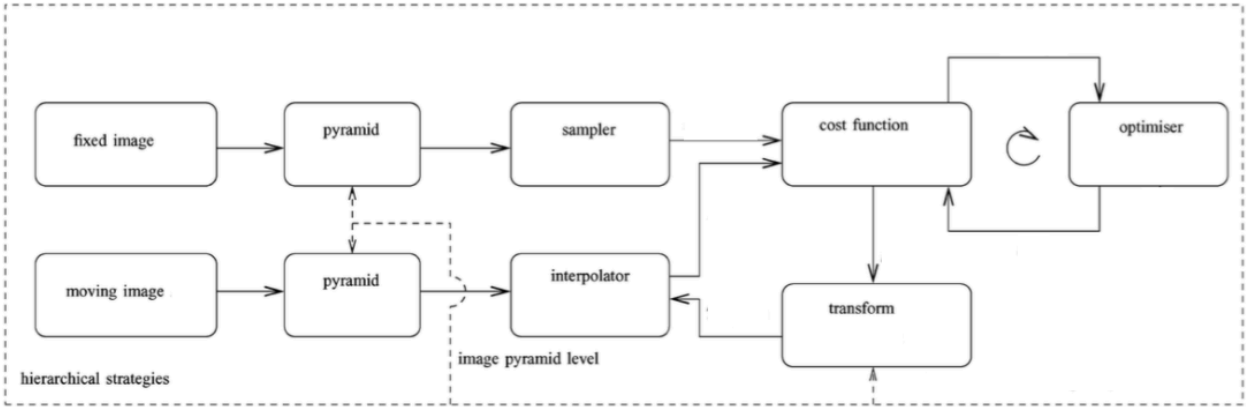

Figure 2: Diagram displaying the components of image registration (adapted from Klein et al). [10] In this case, the fixed image is the processed CT from after the implantation, the moving image is the CT from before, and the final transform is applied to the MRI from before implantation. The Advanced Mattes Mutual information metric is used for rigid and nonrigid registrations

In order to create a successful nonlinear registration between the pre and postoperative scans, the image registration toolbox Elastix is employed (http://elastix.isi.uu.nl/). Elastix is a publicly available program for intensity based medical image registration consisting of a collection of algorithms that are commonly used to solve registration problems.[10] It relies heavily on the

Insight Segmentation and Registration Toolbox (ITK). Figure 2 graphically illustrates the process by which Elastix uses a pyramidal resolution approach, samples the fixed image, and iteratively optimizes the transform based on a certain metric for each pyramidal resolution level. Through a command line interface, a moving image, a fixed image, any masks to be used, an output directory and a parameter file containing the specific details of the registration to be performed are specified.

One transformation method for nonrigid registration is the B-spline. In Elastix, the B-spline is modeled as a 3D weighted sum of B-spline basis functions placed on a uniform control point grid to determine the displacement of the voxels in the transformation. Since this registration task will be challenged with aligning images from modalities that have different contrast properties, Advanced Mattes mutual information will be employed.[11] Mutual information is a statistically based image registration technique derived from probabilistic measures of image intensity rather than making assumptions about the actual intensity values within the images. The Advanced Mattes Mutual Information metric has been optimized for B-spline nonrigid registrations and updated using Parzen window histogram estimates. [11]

2.2 Procedure Outline

In order to bring the MRI into the same space as the brain CT after the implantation procedure some processing needs to be done on the images before the actual registration algorithm is performed. First the excess background is removed, bringing all of the centroids into rough alignment. Then all volumes are brought into rigid alignment with a standard brain atlas. Once in rigid alignment, processing must be done in order to generate a mask for the fixed image and

to generate a fixed image from the post implantation CT that has fewer artifacts and defects. The nonrigid registration is then performed using the CT from before implantation as the moving image and the processed CT from after the implantation as the fixed image. The resulting transformation is then applied to the preoperative MRI.

2.3 Pre-alignment

Three image acquisitions are required for this protocol, one T1 3D gradient echo MRI prior to electrode implantation, one CT prior to implantation, and one thinly sliced CT acquired after implantation in which all of the electrodes are visible. All 3 volumes are resampled to 1mm isotropic resolution regardless of original voxel size, although this is a common acquisition resolution for the 3D MRI.

In order to assist the registration algorithm and improve efficiency, excess background is removed from the MRI and the two CTs, approximately aligning the centroids. This is done by segmenting every voxel in the MRI with an intensity less than 50 into one grouping and everything with an intensity greater than 50 into another group. Moving from the outside in on each edge, in every dimension, if a slice contains only voxels in the lower intensity group, the slice is removed from the cropped volume.

Similarly, the CT volumes are segmented based on voxel intensity. After a 3D Gaussian filter is applied with a standard deviation of 6 voxels, all voxels with intensity lower than -100 are assumed to be in the background, and moving from the outside in, if a slice is found to contain

all voxels less than -100, it is removed. This is done in all directions, removing excess background, and bringing the two CTs into rough alignment with each other and the MRI.

2.4 Rigid registration

Once the excess background has been removed, the three volumes are put into rigid alignment. Because the head can be positioned differently during different scans, all of the volumes are put into alignment with the standardized brain from the Montreal Neurological Institute (MNI) 1mm T1 atlas. Putting the volumes in alignment with an atlas makes it easier to reliably detect the top and bottom of the brain without user interaction and also provides viewing consistency. The MRI scan is placed into rigid alignment with the MNI atlas first. Then the registered MRI is used as the fixed image and the preoperative CT as the moving image. Once those two images are in alignment, the postoperative CT is registered using the newly registered preoperative CT as the fixed image. No mask was used on the fixed or moving images during the rigid registration process. All of the parameters used in the rigid registration are provided in appendix A**.** This registration uses an Advanced Mattes Mutual information metric and a pyramidal registration structure. In order to maintain rigidity, the Euler Transform is used. Background voxels are filled in with values of zero on the MRI if necessary and with -1000 on the CT if necessary.

2.5 Preprocessing

2.5.1 Mask generation

Now that all three volumes are in rigid alignment a mask needs to be generated to tell the registration algorithm where to sample. Voxels in the mask will be selected by extracting the brain, and then limiting them based on their intensity. The brain is extracted from the CT in both

the pre and postoperative cases using the graph search method.[12] This process requires a start and stop slice. The start slice is chosen based on the slice containing the least amount of voxels in the -10 through 100 Hounsfield unit (HU) window in the preoperative CT. This is typically just below the base of the brain, where there is more bone and air in the field of view than water and soft tissue. After finding this minimum, the graph search algorithm begins the extraction with the start slice 5mm above this point or 5 slices higher. Graph search brain extraction is applied for each slice moving upward in the brain until the enclosing area contains less than 2000 voxels. Typically this is the approximate number of voxels that will be contained in the most superior slice of the brain when it is in this orientation. This is then the stopping slice. Now that the starting and stopping slice are found, they can be applied to the postoperative CT as well.

Taking these start and stop slices, the mask for the fixed image is created by extracting the brain from the postoperative CT using graph search and removing all voxels in which the CT has intensity of greater than 100 HU. This limits the image sampler to inside the brain and prevents sampling the electrodes or areas with high intensity artifact.

2.5.2 Fixed image generation

Although the mask can effectively limit sampling in the full resolution image, when a pyramidal registration strategy is employed, features from outside of the masked area can still have an effect on the registration during earlier iterations. This heavy blurring is important in the earlier steps, as it makes the algorithm more robust and usable under different types of implanted brains, and it allows for correction to greater displacements in fewer iterations.[13] However, because a 3D Gaussian filter with a large standard deviation is applied to smooth these features across the

entire image, sometimes unwanted distal features and edges that are present in the post-implantation but not in the pre-implantation image can have a negative effect on the registration. In order to correct for this the post contrast image must be processed prior to nonrigid registration.

Small holes in the skull resulting from the craniotomy, streaking and beam hardening artifacts caused by the electrodes, and the presence of other foreign objects within the field of view are likely to cause problems as they will not be present in the presurgical CT. Figure 3 shows an example of a CT that has undergone nonrigid registration without the correction for skull defects. Extra distortion is noticeable in the region nearest to the edges created by the holes, which are present in only in the post implantation volume.

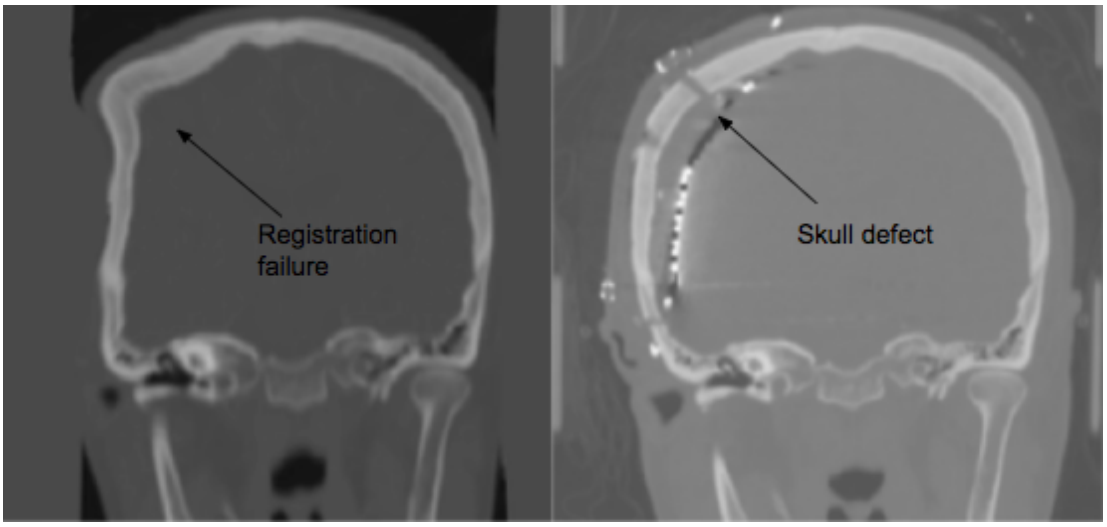

Figure 3: Registration failure resulting from skull defect. The left image shows a coronal slice of an output CT resulting from a nonrigid registration. The image on the right shows the same coronal slice on the post implantation CT that was used as the fixed image during the registration.

Since the skull and the area surrounding the brain is not a part of our volume of interest, it does not need to be considered in the registration algorithm and the irrelevant information that these

features bring can be erased by replacing the skull and all remaining background from the post surgical CT with that of the pre surgical CT so that they match exactly. Given that the rigid registration and brain extraction from the presurgical CT were successful, everything outside of the extracted area on the presurgical CT can be placed in it's respective location on the postoperative CT in a voxel wise replacement.

The effect on the mutual information metric from the artifacts that the electrodes create can be reduced in the generated fixed image as well. To process the volume within the skull on this new fixed image, two masks are first created. One mask is created by taking the original brain mask from the extracted post implantation CT brain and removing all of the voxels outside of the 10 to 100 HU window. Another mask is created based on the extracted brain after performing morphological opening to remove any residual skull or electrodes on the surface, and using the graph search method again to create a sparser mask that does not include the streaking artifacts on the edges. The union of these two masks is taken and morphologically closed. Everything within the skull and not inside this mask is thought to be either influenced by artifact or to be CSF. These voxels are all set to zero. The resulting image has fewer artifacts and less defects from the craniotomy. An example is shown in figure 4.

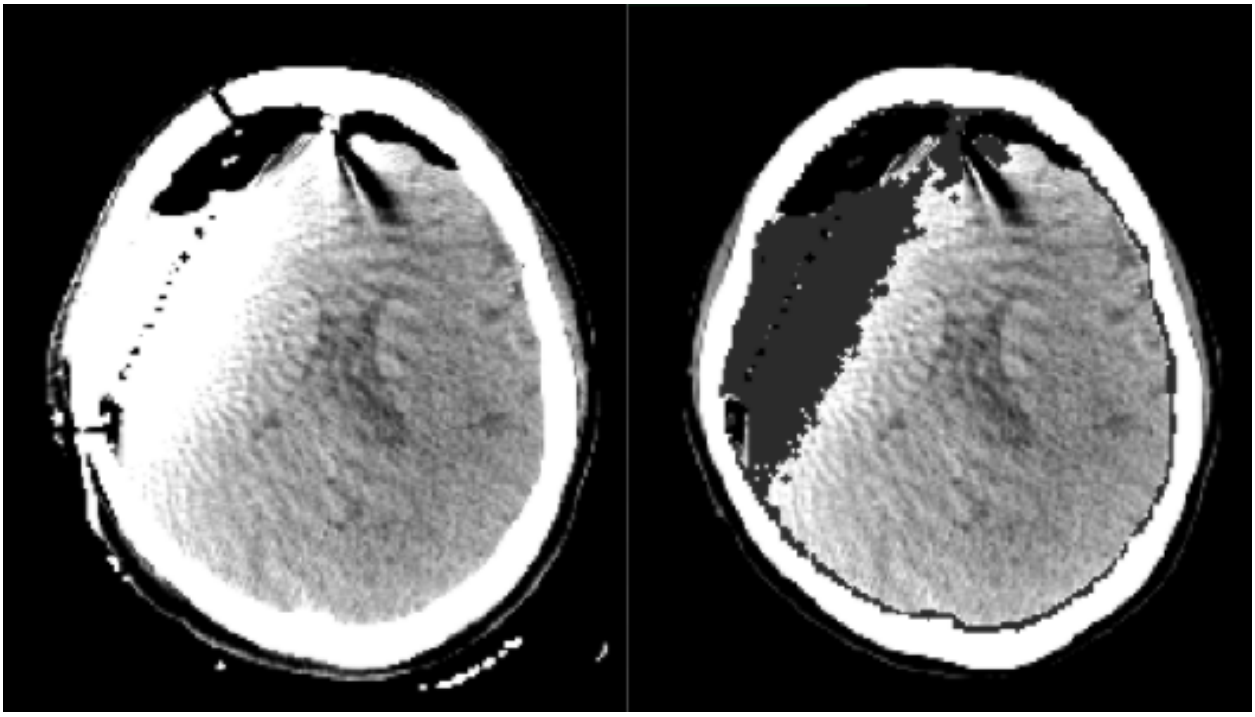

Figure 4: Original post implantation CT on the left and processed image on the right to be used as fixed image in nonrigid registration step

2.6 Nonrigid registration

2.6.1 Registration parameters

Elastix is used to run the nonrigid registration. It uses the image generated above as the fixed image, the mask generated above to limit the region sampled by the algorithm and the pre surgical CT as the moving image. In order to allow for more variable amounts of deformation, a 4 level registration pyramid is used with more smoothing in the axial directions than in the z directions because in almost all cases, the z direction will originally have the lowest resolution before resampling. The metric chosen here is Advanced Mattes Mutual Information because of its ability to handle varying contrast properties in the moving and fixed images and its functionality with a pyramidal structure. A B-spline transformation is used along with a bending energy penalty, weighted at 100 times the mutual information metric. The full parameter file containing all of the parameters involved in the registration can be found in appendix B.

2.6.2 Application of Transformation

After the pre surgical CT has been registered to the post-surgical CT, a transformation file containing all of the information necessary to resample the moving image into the newly registered space will have been generated. Since the MRI is already in rigid alignment with the CT volumes, this transformation file is applied to the MRI, and the MRI is transformed into the new post implantation space.

One final check is also built into the pipeline in which the determinant of the jacobian matrix is computed for each voxel in the field of view. Jacobian determinants greater than one indicate expansion, while those less than one indicate compression. Any determinant less than zero indicates a transformation that would not naturally be seen in medical imaging transformations, and if this exists within the brain, the transformation is invalid and should not be used. If a negative jacobian determinate were to exist anywhere in the field of view, a message would be generated warning the user to carefully investigate before proceeding.

3 Results

3.1 Qualitative results

The registration algorithm was performed on 5 subjects, all of whom had undergone implantation of both surface and depth electrodes in varying locations. They had varying degrees of post surgical brain deformation, and in each case, both a CT and an MRI were acquired prior to surgery and a CT visualizing the electrodes was acquired after the implantation. A single slice depicting the structure of the brain before and after the transformation for one of these subjects is shown in figure 5.

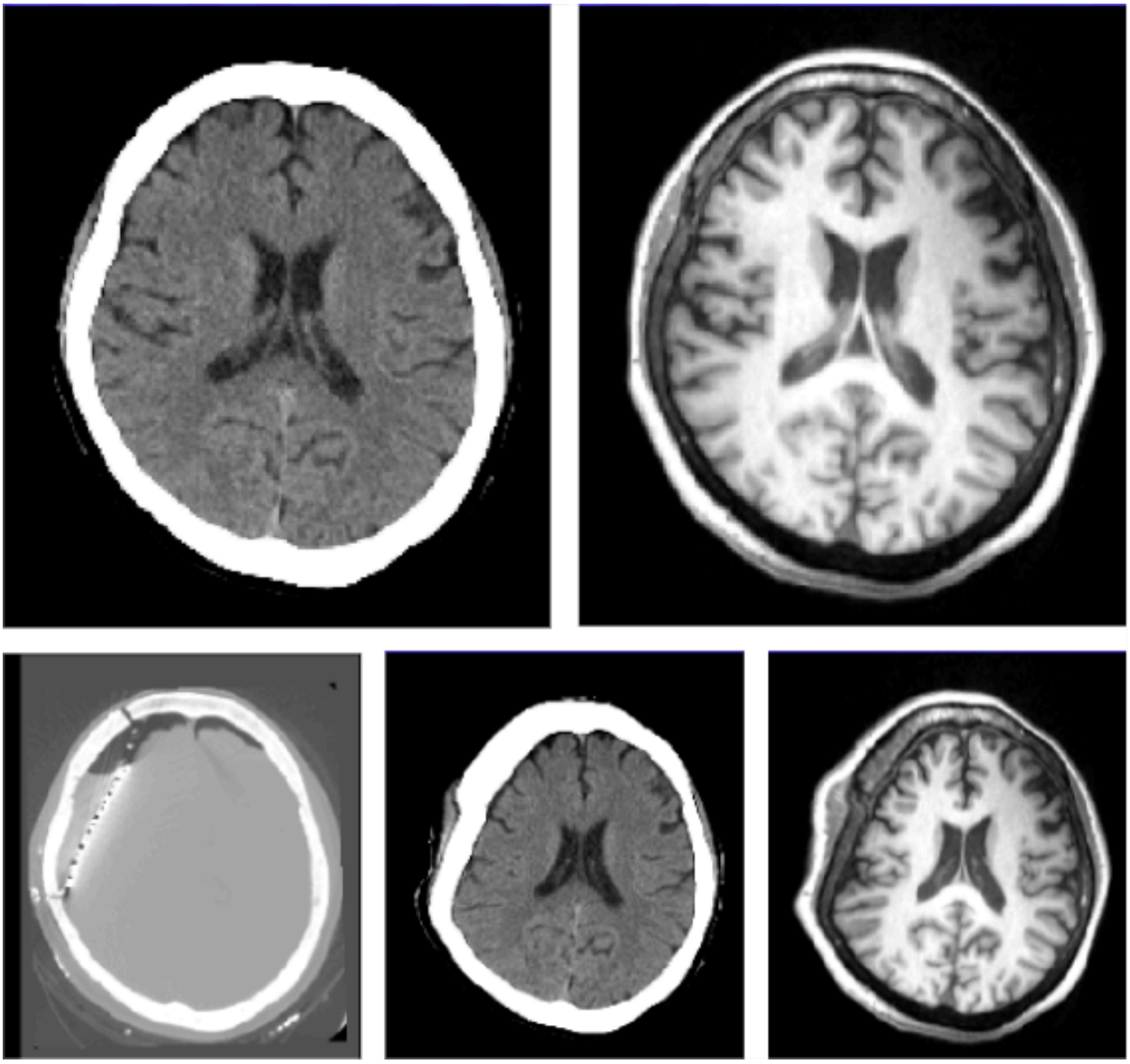

Figure 5: A single slice from one subject as the algorithm is applied. In the top row the original CT and MRI prior to implantation are shown. In the bottom row, the post-implantation CT is shown on the left, the nonrigidly registered CT in the center, and then on the right is the MRI after the transformation has been applied.

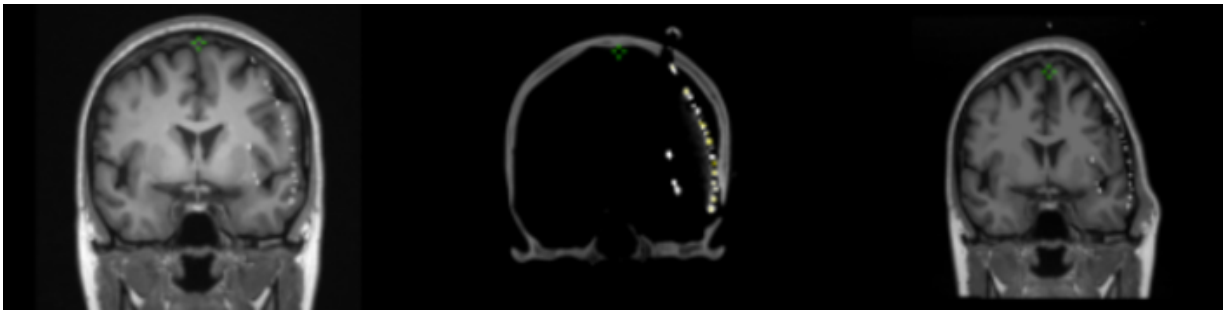

Figure 6: MRI (left, right) with electrodes from CT (middle) before transformation on left and after transformation on the right

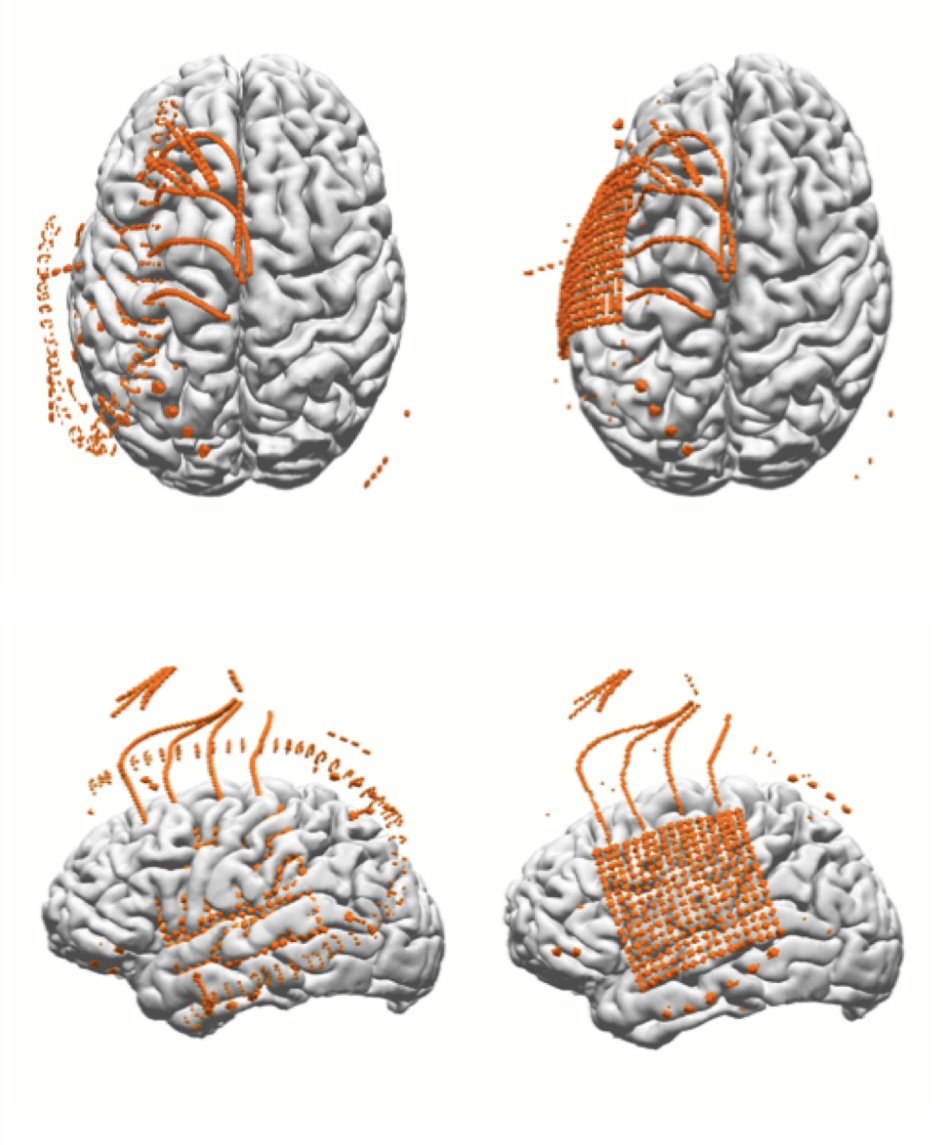

Figure 7: 3D surface renderings of MRI with electrodes before and after application of nonrigid transformation.

Qualitatively, this processing pipeline adequately brought the grids to the surface and aligned the internal structures as shown in figures 5 and 6**.** Figure 7 shows the surface electrodes embedded within the brain before the pipeline and resting on the surface after. Figure 8 shows the misalignment of the ventricles before the pipeline, and the correction that occurs after the pipeline has been run, characterizing a correction for the depth electrodes.

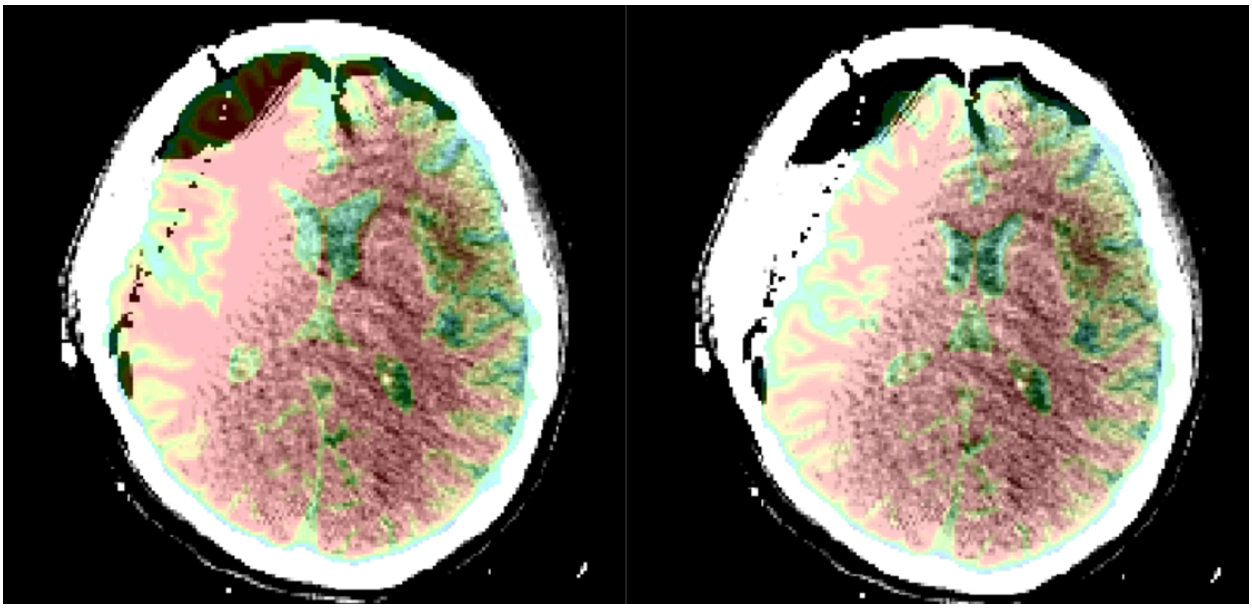

Figure 8: Coregistration of internal brain structures. CT is shown as grayscale background with colored MRI overlaid. Left is before transformation. Right is after transformation.

3.2 Validation

3.2.1 Surface Validation

Validation of the final positioning of the electrode correction in relation to the newly adjusted MRI must be done separately for the surface and depth electrodes. For the surface electrodes, the same transformation was applied to a T1 3D SPGR that was acquired post gadolinium injection. The surface grids were then overlaid on a 3D surface rendering of this volume so that the vasculature was clearly visible both before and after the nonrigid portion of the registration procedure using Curry (Compumedics Neuroscan, Charlotte, NC, USA).[14] Using vascular

landmarks visible in both the 3D surface renderings and the intraoperative photograph shown in figure 9, the relative locations of each of the 6 grid corners visible in the photograph were measured. Using the locations on the photograph as ground truth, the errors given by the surface location on the volume before nonrigid registration and after nonrigid registration were recorded and are available in table 1**.** On average, the warping gave an error reduction of 3mm with a standard deviation of 3mm (P=0.06). A two-tailed t-test was used to check for significance.

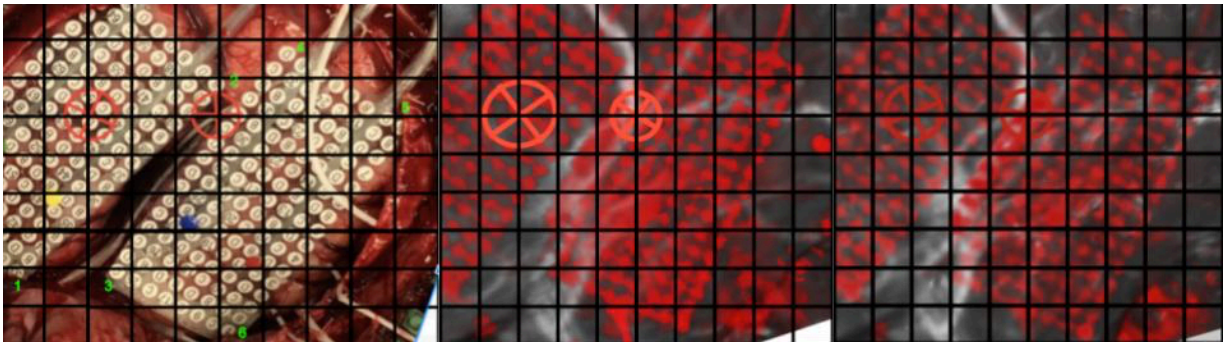

Figure 9: Intraoperative photograph with vascular landmarks as red crosshair and a grid overlay. Center and righthand images are the postcontrast T1 surface renderings before and after the transformation respectively. Red dots indicate electrode locations from the CT

Table 1: Surface electrode error based on comparison to intraoperative photograph.

Corner	Error before NR registration (cm)	Error after NR registration (cm)	Improvement (cm)
1	1.3	0.4	0.9
2	0.7	0.5	0.2
3	0.4	0.1	0.3
4	1.3	0.8	0.5
5	1.6	1.4	0.2
6	1.1	1.2	-0.1
Mean	1.1	0.7	0.3
Std Dev	0.4	0.5	0.3
			P=0.06

3.2.2 Depth Validation

Validation for the depth electrodes is difficult because depth electrodes are only visualized within the imaging. Because of this, the ground truth for depth electrode location must be based on electrophysiology. A blinded neurologist trained to analyze intracranial EEG analyzed the signal from each of the depth electrodes and determined which signals were most likely to be recording from gray matter (as opposed to white matter or CSF). Concurrently, the MRI for each subject, both before and after nonrigid registration, was skull stripped using FSL's brain extraction tool, and automatically segmented into gray matter white matter and CSF using the FSL FAST pipeline (https://fsl.fmrib.ox.ac.uk/fsl/fslwiki). [15] Any electrode for which the majority of its volume was within the gray matter according to this segmentation was said to be in gray matter according to the imaging. The scores for whether or not the imaging correctly identified an electrode to be in gray matter or not in gray matter were calculated for both before and after the nonrigid registration. The results for this method are given in table 2. On average, nonrigid registration gave an improvement in gray matter localization for the depth electrodes of 12.5% ± 2.3% more electrodes correctly identified ($P<0.001$). A two-tailed t-test was used to check for significance.

Table 2: Depth electrode localization scores. Given as ratio of electrode correctly identified as either gray matter or not gray matter.

	Subject1	Subject2	Subject3	Subject4	Subject5	Mean	StDev
Pre-reg score	0.500	0.455	0.625	0.651	0.619	0.570	0.087
Post-reg score	0.625	0.545	0.775	0.767	0.762	0.695	0.104
Difference	0.125	0.091	0.150	0.116	0.141	0.125	0.023
						p=0.000279	

4 Discussion

4.1 Analysis

For the surface validation, errors were smaller nearer to the center of the field of view for both the volume before and after nonrigid registration. This likely has to do with the perspective and the camera angle. Also, this type of analysis makes the assumption that all of these electrodes are in the same plane. In reality the curvature of the brain puts these corners into different planes making this assumption false. Corners five and six are also only partially visible in the photograph. Since corners five and six are impacted by all of these factors, it makes sense that they would both have higher displacement errors both before and after nonrigid registration.

It also follows that the depth electrodes would be better localized based on gray matter signal after nonrigid registration based on visual inspection of the images in figure 8. When the internal structures of the brain are in alignment, this indicates a successful registration in the vicinity of the deep structures of the brain, placing the depth electrodes in the correct locations on the newly transformed MRI volume. It is interesting, however, that although the degree of deformation in the brain varied among the 5 subjects, the improvement in the number of depth electrodes successfully localized to either gray matter or not gray matter (white matter or CSF) was fairly consistent.

4.2 Limitations

Although the requirement for a CT before the implantation of electrodes has not proven to be too limiting, not every patient will have a CT before their surgery. This extra CT causes unwanted exposure to ionizing radiation and an additional medical expense. An ideal pipeline would

minimize the number of scans required to one prior to implantation and one after. Also, the resulting coregistration is much improved using this nonrigid transformation, but the result is still imperfect as shown by the error results seen in this study here and improvements can still be made to diminish these errors.

4.3 Sample Size

In order to be fully analyzed, a larger sample size is needed. Fortunately this is a fully automated tool that can be used to evaluate any patient that has had MRI and CT imaging before implantation and a CT while implanted. There should be no shortage of future subjects on which this can be tested. The presurgical CT requirement can is relatively relaxed, and good results have been observed even with low resolution, and low dose CT scans used for attenuation correction in other studies. Although many steps have been taken to optimize this method, there is the possibility that future versions could present an improvement and further lower the error noted above. Now that a pipeline and a validation method have been developed however, future adjustments and improvements would be easier to implement should they become necessary or desirable.

4.4 Validation methods

Given access to different imaging modalities, validation methods could also be improved. Using an MRI that has been acquired after the implantation procedure as a ground truth for the final registration could present a marked improvement on the validation methods used here. More high quality photographs with standard perspective and more visible landmarks for reference could also provide better validation.

4.5 Efficiency

It should also be noted that this pipeline runs for about 20 minutes without any user interaction on a computer with a 3.7 GHz quad-core processor and 32GB of memory. This should allow for easy incorporation into a clinical workflow. If further efficiency optimizations were implemented, faster processing times could be obtained on less powerful computers, but further validation may be required.

4.6 Expansion

Further studies examining the relationship between the epilepsy foci derived from nonrigid registration compared to the localization derived from the original MRI will prove to be valuable. These along with pathological data attained from subsequent surgical resection specimens could provide more information that reflects the accuracy and efficacy of this method.

Combining this tool with other tools for greater power and automation may have future value as well. Using automated spike detection and finite element models may improve user experience while leading to an even more accurate epileptic focus localization. Other processing and registration techniques that have been used in the past could also be combined with this method for a more versatile product.

5 Conclusion

This automated pipeline effectively corrects for the brain shift caused by the surgical implantation of intracranial electrodes on the surface and deep within the brain. It brings a nondeformed brain into the space of the brain depicted in the post-surgical CT such that the

electrodes are now in appropriate locations in relation to the newly deformed volume. From the sample observed here, there is a significant improvement in the localization of both the surface and the depth electrodes in relation to the MRI.

References

1. Fisher, Robert S. et al. "Epileptic Seizures And Epilepsy: Definitions Proposed By The International League Against Epilepsy (ILAE) And The International Bureau For Epilepsy (IBE)". *Epilepsia* 46.4 (2005): 470-472.

2. Cdc.gov. (2017). *Data and Statistics | subsection title | section title | site title*. [online] Available at: https://www.cdc.gov/epilepsy/data/index.html [Accessed 7 Sep. 2017].

3. Fisher, Robert S. et al. "ILAE Official Report: A Practical Clinical Definition Of Epilepsy". *Epilepsia* 55.4 (2014): 475-482. Web. 9 June 2017.

4. Sirven, Joseph et al. "Evaluation And Management Of Drug-Resistant Epilepsy". *Uptodate.Com*, 2017, https://www.uptodate.com/contents/evaluation-and-management-of-drug-resistant-epilepsy.

5. Englot, Dario J. et al. "Factors Associated With Failed Focal Neocortical Epilepsy Surgery". *Neurosurgery* 75.6 (2014): 648-656.

6. Hashiguchi, Kimiaki et al. "Correlation Between Scalp-Recorded Electroencephalographic And Electrocorticographic Activities During Ictal Period". *Seizure* 16.3 (2007): 238-247.

7. Nimsky, Christopher et al. "Quantification Of, Visualization Of, And Compensation For Brain Shift Using Intraoperative Magnetic Resonance Imaging". *Neurosurgery* 47.5 (2000): 1070-1080.

8. Akalin Acar, Zeynep, and Scott Makeig. "Effects Of Forward Model Errors On EEG Source Localization". *Brain Topography* 26.3 (2013): 378-396.

9. Dykstra, Andrew R. et al. "Individualized Localization And Cortical Surface-Based Registration Of Intracranial 7Electrodes". *NeuroImage* 59.4 (2012): 3563-3570.

10. Klein, S. et al. “Elastix: A Toolbox For Intensity-Based Medical Image Registration". *IEEE Transactions on Medical Imaging* 29.1 (2010): 196-205.

11. Mattes D. et al. “Nonrigid multimodality image registration”. *Medical Imaging* 4322 (2001): 1609-1620.

12. Pedoia, Valentina, and Elisabetta Binaghi. "Automatic MRI 2D Brain Segmentation Using Graph Searching Technique". *International Journal for Numerical Methods in Biomedical Engineering* 29.9 (2012): 887-904.

13. Lester, H. and Arridge, S. (1999). A survey of hierarchical non-linear medical image registration. *Pattern Recognition*, 32(1), pp.129-149.

14. Curry. Charlotte, NC, USA: Compumedics Neuroscan.

15. FSL <https://fsl.fmrib.ox.ac.uk/fsl/fslwiki>

Appendix A: Parameter text file for rigid registration

```
(FixedInternalImagePixelType "float")
(MovingInternalImagePixelType "float")
(FixedImageDimension 3)
(MovingImageDimension 3)
(UseDirectionCosines "true")
// *************** Main Components **************************
(Registration "MultiResolutionRegistration")
(Interpolator "BSplineInterpolator")
(ResampleInterpolator "FinalBSplineInterpolator")
(Resampler "DefaultResampler")
(FixedImagePyramid "FixedSmoothingImagePyramid")
(MovingImagePyramid "MovingSmoothingImagePyramid")
(Optimizer "AdaptiveStochasticGradientDescent")
(Transform "EulerTransform")
(Metric "AdvancedMattesMutualInformation")
// ***************** Transformation **************************
(AutomaticScalesEstimation "true")
(AutomaticTransformInitialization "true")
(HowToCombineTransforms "Compose")
// ****************** Similarity measure *********************
(NumberOfHistogramBins 64)
(ErodeMask "false")
```

```
// ******************** Multiresolution **********************

(NumberOfResolutions 4)

(ImagePyramidSchedule 12 12 4 6 6 2 3 3 1 1 1 1)

// ******************* Optimizer ****************************

(MaximumNumberOfIterations 5000)

(MaximumStepLength 1.0)

(RequiredRatioOfValidSamples 0.05)

// **************** Image sampling **********************

(NumberOfSpatialSamples 5000)

(NewSamplesEveryIteration "true")

(ImageSampler "RandomCoordinate")

// ************* Interpolation and Resampling ****************

(BSplineInterpolationOrder 1)

(FinalBSplineInterpolationOrder 3)

(DefaultPixelValue 0)

(WriteResultImage "true")

(ResultImagePixelType "short")

(ResultImageFormat "nii.gz")
```

Appendix B: Parameter file for nonrigid registration

```
// ********** Image Types
(FixedInternalImagePixelType "float")
(FixedImageDimension 3)
(MovingInternalImagePixelType "float")
(MovingImageDimension 3)
// ********** Components
(Registration "MultiMetricMultiResolutionRegistration")
(Interpolator "BSplineInterpolator")
(ResampleInterpolator "FinalBSplineInterpolator")
(Resampler "DefaultResampler")
(FixedImagePyramid "FixedSmoothingImagePyramid")
(MovingImagePyramid "MovingSmoothingImagePyramid")

(Optimizer "AdaptiveStochasticGradientDescent")
(Transform "BSplineTransform")
(Metric "AdvancedMattesMutualInformation" "TransformBendingEnergyPenalty")
(Metric0Weight 1)
(Metric1Weight 100)
// ******************** Multiresolution **********************
// Total number of resolutions
(NumberOfResolutions 4)
(ImagePyramidSchedule 12 12 4 6 6 2 3 3 1 1 1 1)
```

```
// ********** Transform
(AutomaticTransformInitialization "true")
(AutomaticScalesEstimation "true")
(HowToCombineTransforms "Compose")
// ********** Optimizer
(MaximumNumberOfIterations 5000 5000 5000 15000)
(AutomaticParameterEstimation "true")
(UseAdaptiveStepSizes "true")
(ASGDParameterEstimationMethod "Original")
// ********** Metric
(NumberOfHistogramBins 64)
(FixedLimitRangeRatio 0.0)
(MovingLimitRangeRatio 0.0)
(FixedKernelBSplineOrder 1)
(MovingKernelBSplineOrder 3)
(UseFastAndLowMemoryVersion "true")
(WriteTransformParametersEachIteration "false")
(WriteTransformParametersEachResolution "false")
(WriteResultImageAfterEachResolution "false")
(WritePyramidImagesAfterEachResolution "false")
(WriteResultImage "true")
(ShowExactMetricValue "false")
```

```
(ErodeMask "false")

(UseDirectionCosines "true")

// ********** Image sampling **********

(ImageSampler "RandomCoordinate")

(NumberOfSpatialSamples 5000)

(NewSamplesEveryIteration "true")


// ********** Interpolation and Resampling **********

(BSplineInterpolationOrder 1)

(FinalBSplineInterpolationOrder 3)

(DefaultPixelValue 0)

(ResultImageFormat "nii")
```

Publishing Agreement

It is the policy of the University to encourage the distribution of all theses, dissertations, and manuscripts. Copies of all UCSF theses, dissertations, and manuscripts will be routed to the library via the Graduate Division. The library will make all theses, dissertations, and manuscripts accessible to the public and will preserve these to the best of their abilities, in perpetuity.

I hereby grant permission to the Graduate Division of the University of California, San Francisco to release copies of my thesis, dissertation, or manuscript to the Campus Library to provide access and preservation, in whole or in part, in perpetuity.

Author Signature Ben Spindel Date 9/11/2017